Rheological Characterization of a New Type of Colloidal Dispersion Based on Nanoparticles of Gelled Oil

ARTICLE *in* THE JOURNAL OF PHYSICAL CHEMISTRY B · AUGUST 2009

Impact Factor: 3.3 · DOI: 10.1021/jp905260s · Source: PubMed

Rheological Characterization of a New Type of Colloidal Dispersion Based on Nanoparticles of Gelled Oil

Plamen Kirilov, Fabienne Gauffre, Sophie Franceschi-Messant, Emile Perez,* and Isabelle Rico-Lattes

Laboratoire des I.M.R.C.P. UMR 5623 CNRS, Université Paul Sabatier, 31062 Toulouse, France

Received: June 04, 2009; Revised Manuscript Received: July 01, 2009

The rheological properties of a new type of colloidal dispersion based on nanoparticles of gelled oil have been characterized. The nanoparticles (mean diameter ~ 250 nm) were viscoelastic droplets of dicaprylyl ether gelled by 12-hydroxystearic acid (HSA) and were stabilized in aqueous solutions by cetyltrimethylammonium bromide. The effects of the volume fraction of the dispersed organogel phase and of the organogelator concentration upon viscoelasticity of the dispersion were investigated and compared to the corresponding emulsion (without HSA). The shear viscosity of the dispersions of organogel droplets and the elastic and viscous moduli (G' and G'') were found to increase when the proportion of organogelator was increased. More surprisingly, the shear-thinning behavior was also more pronounced. The rheological behavior of the dispersions could be explained by strong interactions between some gelled particles. This hypothesis was supported by electron microscopy observations showing some particles bridged together by ribbons of HSA fibers.

1. Introduction

Physical organogels are produced when a minor component forms an extended three-dimensional network through microphase separation or molecular interactions in an organic liquid. These organogels, which usually consist of less than 2 wt % of low-molecular-mass organic gelator or organogelator (LMOG) and a liquid,[1,2] are also potentially attractive templates[3−6] due to the 10−100 nm (monodisperse in many cases) cross sections of the fibers that make up their self-assembled fibrillar networks (SAFINs).[7,8] The intermolecular interactions can be of different origins including hydrogen bonding,[9−13] van der Waals forces,[14−17] $\pi-\pi$ stacking,[18−20] donor−acceptor interactions,[21,22] ionic or organometallic coordination bonding,[23−25] or a combination of these. Organogels have become the subject of increasing fundamental and technological interest.[26,27] They are readily obtained by dissolving a small amount of the LMOG at high temperature and cooling the solution below a characteristic gelation transition temperature, known as T_{gel}. Empirically, T_{gel} is the temperature below which flow is no longer discernible over a long period. It depends on the concentration of the organogelator, the properties of the organic liquid (polarity, viscosity, etc.), and in some cases, the cooling protocol of the solution/sol.[28] The physical network forms upon cooling, leading to a thermally reversible organic gel-like material characterized by a significant elasticity.[29,30]

Very recently, we proposed an original process to produce stable dispersions of monodisperse nanoparticles of organogel in water with a very narrow polydispersity.[31,32] The colloidal particles of organogel could be considered as an alternative to solid particles, emulsions, and liposomes in cosmetic and pharmaceutical preparations.[33−36] These dispersions are elaborated by hot emulsification and cooling at room temperature in the presence of a polymer or surfactant as stabilizer.[31]

The present paper explores the rheological behavior of such colloidal dispersions of organogel nanoparticles under steady and oscillatory shear flow. The organogel phase was made from dicaprylyl ether, an emollient oil used in cosmetics, and 12-hydroxystearic acid (HSA) as the organogelator. Cetyltrimethylammonium bromide (CTAB) was used as an emulsifier and stabilizer of the organogel nanoparticles in water.

2. Experimental Section

2.1. Chemicals. 12-Hydroxystearic acid (HSA) with a purity of 99% was obtained from Casid (Caschem, U.S.). Dicaprylyl ether (>96.5%) and soybean oil (>95%) were obtained from Sigma-Aldrich and Capric/Caprylic triglyceride (55/45%) from Cognis (France). Dodecyl/pentadecyl benzoate (Witconol TN, 95%) was bought from Witko (U.K.) and cetyltrimethylammonium bromide (CTAB, >98%) from Merck. Distilled water was used for the preparation of the emulsions and the corresponding dispersions.

2.2. Gel Preparation. Gel samples were prepared by dissolving the desired weight percentage of HSA (1−15 wt %, based on oil) in oil. For a complete dissolution of HSA, the mixture was homogenized (75 °C, 5 min) by ultrasound (Vibra Cell, Bioblock Scientific with a titanium probe, 20 kHz, 600 W) and cooled at room temperature to form a solid, translucent gel.

2.3. Emulsification and Dispersion Preparation. For all the experiments, the HSA was considered as an oil additive, and consequently its weight percentage was based only on the oil phase and not on the total weight of the dispersion. For ease of comparison between the emulsion (without HSA) and the dispersion, the percentage weights of all the other ingredients were based on the total weight without the HSA.

Water solutions containing the stabilizing agent (CTAB, 1.6 wt %) were added to the previously obtained organogel or to a pure oil phase to obtain the desired volume fraction ϕ (volume of the organic phase over the total volume). The mixture was then heated in an oven at 75 °C (which is above the melting

* To whom correspondence should be addressed. E-mail: perez@chimie.ups-tlse.fr.

10.1021/jp905260s CCC: $40.75
Published on Web 07/22/2009

temperature of the gels) for 20 min and melted to an oily layer at the surface of the solution. Then, the hot mixture (75 °C) was emulsified by sonication (20 kHz, 600 W) for 10 min. For this study, we decided to keep the sonication conditions constant for all the experiments to limit the number of parameters influencing the preparation process. The emulsion thus formed was then cooled at room temperature, leading to a dispersion of organogel particles. The particle diameters were determined by dynamic light scattering (Malvern, Zetasizer 3000HSA) before and after the rheological measurements, to check that there was no significant change in their size during the experiments.

2.4. Rheological Experiments. Oscillatory shear and viscosity measurements were conducted in a stress-controlled rheometer (TA AR1000) system which, depending on the viscosity of the sample, used a cone-and-plate geometry with a cone angle of 2°, 47 μm in truncation, and a diameter of 20 mm, or a cone-and-plate geometry with a cone angle of 2°, 61 μm in truncation, and a diameter of 60 mm. To prevent dehydration from the solution, a thin layer of low-viscosity silicone oil (the viscoelastic response of the sample was not affected by this layer) was placed on the top of the measuring unit. The rheometer was equipped with a Peltier plate that controlled temperature within 0.1 °C of the set value. All rheological experiments were conducted at a temperature of 25 °C. For each measurement, at least two tests were carried out. The reproducibility of an experimental run with a new sample solution was usually better than ±5%.

The viscosity measurements were conducted over an extended range of shear rates (0.03−100 s^{-1}) using a flow procedure (steady-state flow mode). The shear rate dependence of the viscosity was usually monitored as a function of increasing shear rate. Between measurements, the sample was allowed to equilibrate for some time before the experiments started.

All oscillatory shear experiments were carried out within the linear viscoelastic regime, where the dynamic elastic modulus (G') and viscous modulus (G'') are independent of the strain amplitude. The oscillating sweep measurements were performed in the frequency (f) domain of 0.01−30 Hz with an imposed stress of 0.2 Pa.

2.5. Dynamic Light-Scattering Measurements. Dynamic light scattering (DLS) was performed on a Malvern Instruments Zeta Sizer 3000 HSA, using a He−Ne laser (633 nm), at a scattering angle of 90° and at 25 ± 1 °C. The mean hydrodynamic diameter of the nanoparticles was determined using the software provided by Malvern Instruments. The Contin model was applied to obtain size data. All autocorrelation function fits were checked and found to be in accordance with the experimental data. All measurements were obtained from a mean of diluted samples (20 mg of dispersion in 10 mL of distilled water). The accuracy was ±10 nm.

2.6. Transmission Electron Microscopy (TEM) and Freeze Fracture Transmission Electron Microscopy (FF-TEM). The morphology of the particles was examined by TEM (JEOL JEM-1200EX, 80 kV). Diluted samples (5 mg of dispersion in 10 mL of distilled water) were deposited on a 400 mesh carbon film copper grid for 1 min. Then the excess sample solution was removed, and samples were stained with a uranyl acetate solution (1 wt %).

For the FF-TEM investigation, a small quantity (5 μL) of each sample was placed in a sandwich aluminum support (hole Φ = 3 mm) and was frozen in a HPM 010 machine (Bal-Tec) under a pressure of 2100 bar. The specimens thus prepared were transferred to a freeze fracture unit (BAF 400T Bal-Tec) and fractured by a knife at 77 K with a residual pressure of 1.33 10^{-5} Pa. The fractured faces were etched for 10 min at 173 K prior to shadowing. Subsequently, the etched surfaces were shadowed with 2 nm of Pt at a 45° angle to the plane of the sample followed by 20 nm of carbon (at a 90° angle) by electron beam evaporation gun. The resulting replicas were washed in a 10% graded acetone series, rinsed in deionized water, and then collected on 400 mesh grids. Transmission electron microscopy (TEM) was performed on a Zeiss TEM omega 912 operated at 120 kV with images recorded with a Proscan SS-CCD (1k × 1k).

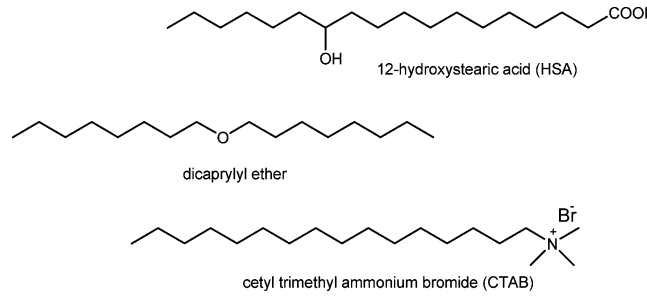

Figure 1. Chemical structures of the various components.

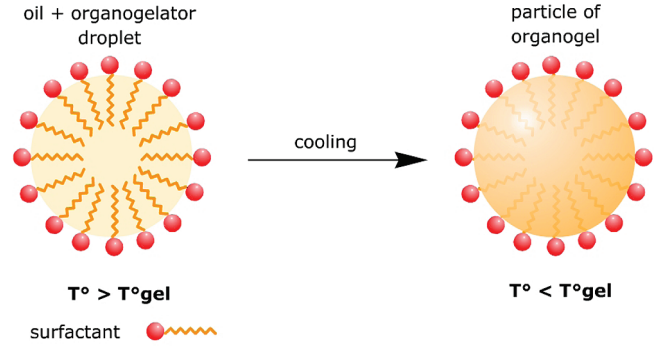

Figure 2. Concept of the elaboration of the gelled nanoparticle as an aqueous dispersion.

3. Results and Discussion

3.1. Dispersions of Organogel Particles. In typical experiments, an aqueous stock solution containing 1.6% CTAB (corresponding viscosity ∼ 1.2 10^{-3} Pa·s at 25 °C[37]) and an organogel made of dicaprylyl ether containing different amounts of 12-hydroxystearic acid as organogelator were both heated above the T_{gel} of the organogel and vigorously emulsified by sonication. The chemical structures of the different ingredients are shown in Figure 1. The organic gelled phase obtained after cooling at room temperature formed dispersed particles of diameter ∼250 nm (polydispersity index: 0.18) as determined by dynamic light scattering. With lower concentrations of CTAB, stable systems could not be obtained. The composition of the samples is described by the weight percentage of HSA present in the oil phase and by ϕ, the volume fraction of the dispersed phase (oil) in the dispersion or the emulsion. Note that, in the present study, samples with or without HSA heated at T > 75 °C (i.e., above the T_{gel} of the gelled nanoparticles) were in the emulsion state (ungelled dispersed phase). The organogel nanoparticle elaboration process is sketched in Figure 2.

3.2. Flow Measurements. ***3.2.1. Influence of the Organogelator Concentration.*** We investigated the rheology of different organogel nanoparticle dispersions for various concentrations of HSA in the oil phase. Figure 3 shows the flow

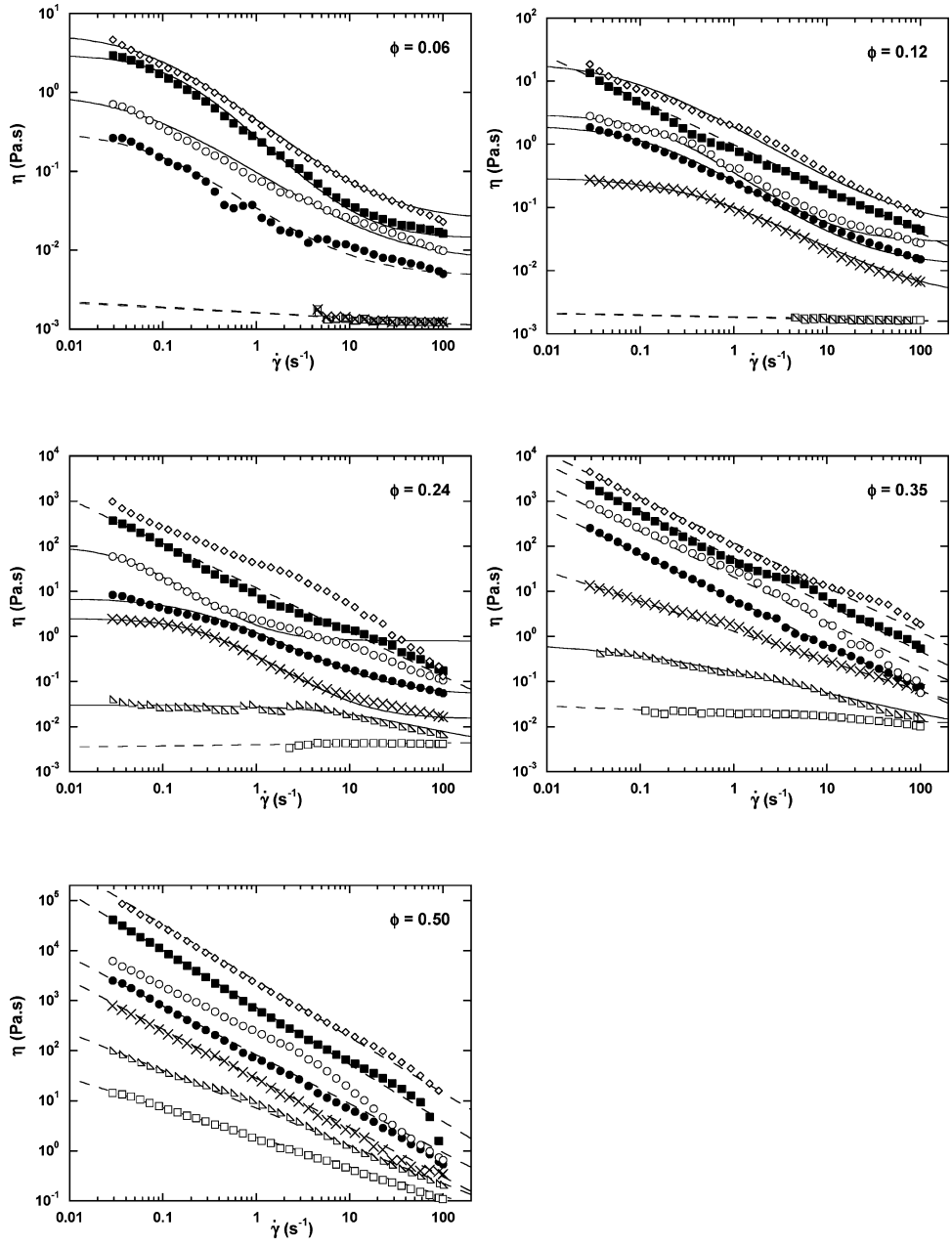

Figure 3. Influence of the oil content in HSA on flow curves for the dispersions of oil droplets and organogel particles at various ϕ (25 °C): (□) 0% HSA; (Δ) 1.5% HSA; (×) 3% HSA; (●) 6% HSA; (○) 9% HSA; (■) 12% HSA; (◇) 15% HSA; (- - -) fit by a power-law model; (—) fit by the Cross law.

curves of samples $\phi = 0.06$, 0.12, 0.24, 0.35, and 0.5 at various weight percentages of HSA in the oil phase (0, 1.5, 3, 6, 9, 12, and 15% HSA). For all the values of the volume fraction, increasing the percentage of HSA from 0 to 15% led to an increase of the shear viscosity by 2−6 orders of magnitude relative to the emulsion (no HSA). This effect was slightly more pronounced at higher values of the volume fraction. For instance, at $\dot{\gamma} = 10\ s^{-1}$, it was of 2 orders of magnitude at $\phi = 0.06$ and of 3 orders of magnitude at $\phi = 0.50$. Increasing the weight percentage of HSA also led to an increase in non-Newtonian behavior which in the present case corresponds to a decrease of the viscosity by increasing of the shear rate. In particular, the emulsion (no HSA) showed Newtonian behavior up to $\phi = 0.35$, whereas with 6% HSA significant non-Newtonian behavior was already observed for dispersions of organogel droplets at $\phi = 0.06$.

When possible, the flow curves were fitted by the Cross model[38] (full line) or by a power-law model[39,40] (dotted lines), using the following equations

$$\text{Cross model:} \quad \eta = \eta_\infty + (\eta_0 - \eta_\infty)/(1 + (K\dot{\gamma})^m) \tag{1}$$

$$\text{power-law model:} \quad \eta = A\dot{\gamma}^{n-1} \tag{2}$$

where η_0 and η_∞ are the low and high shear viscosities, respectively, K and A are constants, and n is commonly referred to as the power-law index. Note that in the intermediate regime, i.e., $\eta \ll \eta_0$ and $\eta \gg \eta_\infty$, the Cross model is reduced to a power-law model with $m = 1 - n$.[38] Numerous experimental data could

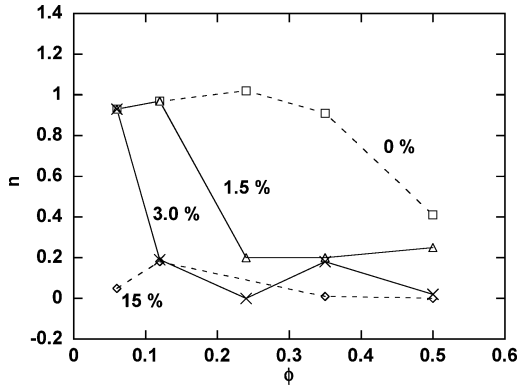

Figure 4. Power-law indices plotted against volume fraction for different organogelator contents in the oil phase: (□) 0% HSA; (Δ) 1.5% HSA; (×) 3% HSA; (◇) 15% HSA. Full and dotted lines are merely guides for the eyes.

be accurately adjusted. The power-law indices extracted from the fits by eq 1 or 2 for the emulsion (no HSA) and gelled nanoparticle dispersions at 1.5, 3, and 15% plotted against the volume fraction are shown in Figure 4. Values close to unity characterize Newtonian behavior and $n < 1$ shear-thinning fluids. It appears clearly from Figure 4 that the sharp transition from Newtonian to shear-thinning behavior shifted to lower volume fraction ϕ when the HSA concentration was increased. Finally, at the highest HSA weight percentage (15%), shear-thinning was observed in the whole range of volume fractions studied.

All these results clearly demonstrate that the HSA concentration has a strong influence on the rheology of these systems. Not only the value of the viscosity but also the way these dispersions flow (Newtonian versus non-Newtonian) are sharply modified. Increasing the amount of HSA in dicaprylyl ether in the range 0−15% changes the viscoelasticity of the oil phase from purely fluid to a nonflowing solidlike gel. In the case of emulsions and dispersions of viscoelastic particles, the viscoelasticity of the dispersed phase can strongly influence the flow properties of the dispersion.[41−43] This is known to occur for concentrated dispersions, when particles undergo deformation under flow. In the present case, at $\phi = 0.50$, this effect cannot be totally excluded. However, the effect of the organogelator upon the shear viscosity was significant at volume fractions as low as $\phi = 0.06$, which cannot be attributed to changes in the viscoelasticity of particles.

In standard droplet dispersions, two different processes can produce shear-thinning: (i) the disturbance of interparticle spacing from equilibrium (e.g., formation of strings of particles) and (ii) droplet deformation.[44] Particularly, hard spheres—such as silica spheres—stabilized with a charged surfactant are expected to undergo a transition from Newtonian to shear-thinning behavior only at concentrations approaching or above the colloidal glass transition[45] ($\phi = 0.58$). Since the spatial distribution of particles should not depend upon the organogelator load, it could be expected here that shear-thinning would result from droplet deformation. However, the present investigation showed that the transition from Newtonian to shear-thinning behavior arose at lower volume fraction when the droplets became harder (or equivalently when the amount of HSA was increased), the hardest droplets exhibiting shear-thinning at concentrations as low as $\phi = 0.06$.

Dilute dispersions in simple fluids generally obey the law of Krieger−Dougherty (see later), which expresses the shear viscosity as a function of ϕ. However, in the case of organogel particles (not displayed), the experimental data could not be satisfactorily fitted by this law.

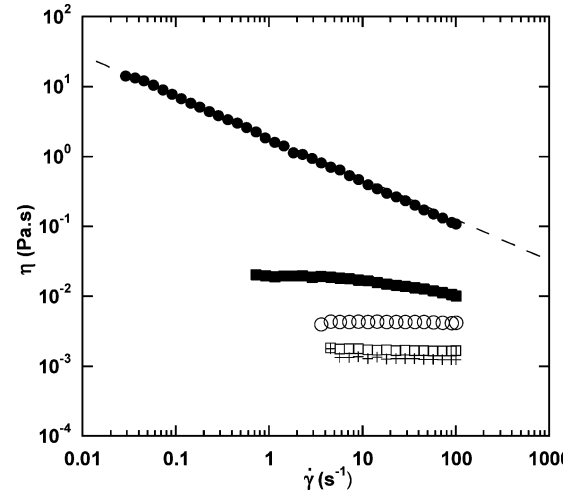

Figure 5. Flow curve of the emulsions (system without HSA) at various volume fractions (25 °C): (+) $\phi = 0.06$; (□) $\phi = 0.12$; (○) $\phi = 0.24$; (■) $\phi = 0.30$; (●) $\phi = 0.50$. The dotted line represents the power-law fit of experimental data for $\phi = 0.50$.

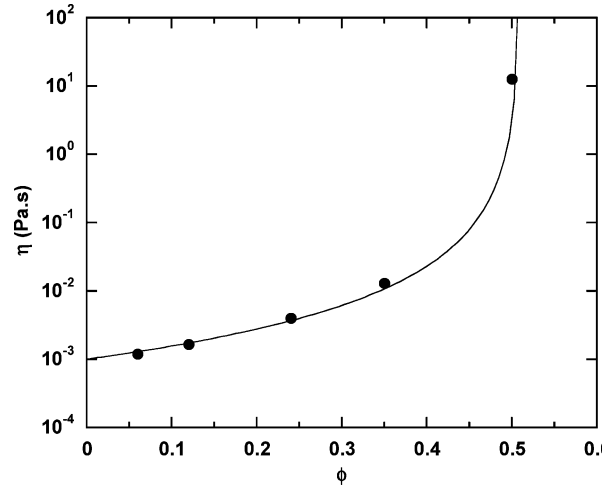

Figure 6. Effect of the volume fraction on the dynamic flow viscosity for the emulsion (no HSA). All viscosity values are measured at shear stress $\sigma = 0.5$ Pa (25 °C). The solid line represents the fit by the Krieger−Dougherty equation.

3.2.2. Emulsion of Dispersed Droplets. We investigated the flow properties of the emulsions either with no HSA or in the presence of the organogelator but above the melting temperature. Figure 5 displays the flow curves for the emulsion (no HSA) at various values of ϕ between $\phi = 0.06$ and $\phi = 0.50$. In comparison with other emulsions in water,[46] the shear viscosity is relatively high (up to 10 Pa·s at $\phi = 0.5$). This is probably due to the small size of the droplets and the narrow size dispersion. Up to $\phi = 0.24$, the emulsion exhibited Newtonian behavior in the range of shear rates studied. Very slight shear-thinning appeared at $\phi = 0.30$ and became much more pronounced at $\phi = 0.50$. The flow curve at $\phi = 0.50$ was fitted by a power law, giving a power-law index $n = 0.59 \pm 0.01$. A clear increase of the shear viscosity with increasing volume fraction of the oil phase was observed. The values of the shear viscosity taken at $\sigma = 0.5$ Pa were extracted from the flow experiments and are shown in Figure 6. A sharp increase of the viscosity is observed at larger values, with a limiting value of the volume fraction around 0.5. The experimental data are satisfactorily fitted by the Krieger−Dougherty equation

$$\eta = \eta_s.(1 - \phi/\phi_m)^{-[\eta]\phi_m} \quad (3)$$

where η_s is the viscosity of the continuous phase. The adjustable parameters of the fit are ϕ_m and $[\eta]$: ϕ_m corresponds to the maximum packing fraction (the fraction at which the particles start to jam-up); the other parameter $[\eta]$ is the intrinsic viscosity (i.e., the dilute limit of the increment per unit particle volume fraction divided by the solvent viscosity). The values given by the fit for the emulsion of dicaprylyl ether in water were $\phi_m = 0.51 \pm 0.01$ and $[\eta] = 4.0 \pm 0.7$. In comparison to other emulsions, the value obtained here for ϕ_m is relatively small. This is most probably due to electrostatic repulsion between droplets induced by the cationic surfactant CTAB as well as to the narrow size distribution.[47,38] The product $[\eta]\phi_m = 2.0 \pm 0.5$ is within the range of values commonly obtained for various dispersions (typically 1.3−2.8).[48]

At temperatures above the melting temperature of the organogel (about 70 °C), the droplets were ungelled. We investigated the rheology of the emulsions obtained by melting the droplets at 70 °C. Figure 7 displays the flow curves for the emulsions formed with 9% HSA at 70 °C for various values of ϕ. These flow curves are almost identical to those obtained for the emulsion with no organogelator (see Figure 5).

3.3. Oscillatory Measurements. Oscillatory measurements were also performed as a function of the shear frequency. The elastic (G') and viscous (G'') moduli at $\phi = 0.24$ are shown in Figure 8b for various organogelator contents (3%, 6%, 15%) and are to be compared to the case of the emulsion (no HSA), which is presented separately for the sake of clarity (see Figure 8a). The oscillatory measurements were carried out at a low deformation rate (1%). Figure 8 reveals the following features: (i) the elastic and viscous moduli significantly increased when the amount of organogelator was increased; (ii) the emulsion, and the dispersions of organogel droplets with 3% and 6% HSA, were predominantly viscous in that their viscous modulus (G'') was higher than their elastic modulus (G') over most of the frequency range investigated. Conversely, for dispersions with 15% HSA, a gel-like behavior ($G' > G''$) was observed over the entire frequency range. The increase in the modulus values together with the appearance of a gel behavior with increasing organogelator concentration can be attributed either to increased viscoelasticity of the continuous phase or to a higher elasticity of the droplets. Oscillatory measurements were also performed under the same conditions on the pure organogel phase for different amounts of HSA. Contrary to the case for the dispersions, the elastic and viscous moduli were independent of the frequency (data not shown). The value of the frequency-independent moduli as a function of HSA content is reported Figure 9. As expected, both moduli increased as the HSA content increased from 0 to 15%. However, this increase was found to be relatively modest (about one decade both for G' and for G'') compared with the increases found for the dispersions (over four decades). These results again suggest that

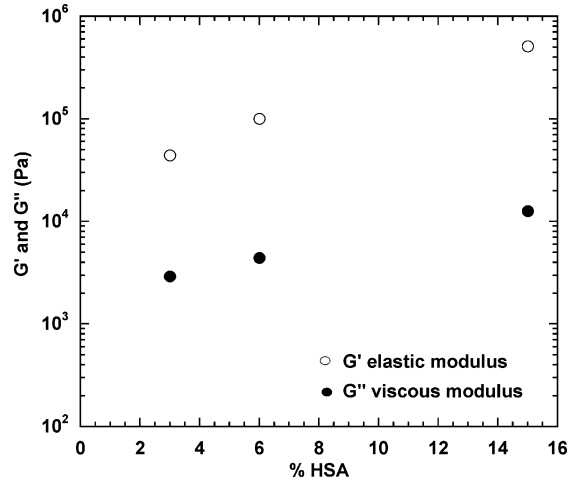

Figure 9. Influence of the HSA contents on the elastic and viscous moduli of the pure organogel phase. Imposed stress $\sigma = 0.2$ Pa (25 °C).

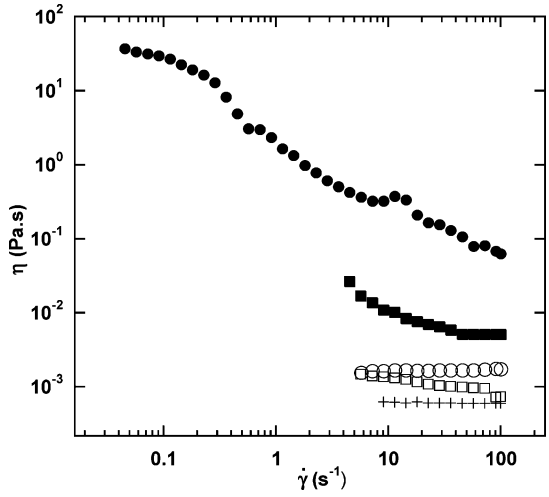

Figure 7. Flow curve of the emulsions ($T = 70$ °C) for particles containing 9% HSA, at various volume fractions: (+) $\phi = 0.06$; (□) $\phi = 0.12$; (○) $\phi = 0.24$; (■) $\phi = 0.30$; (●) $\phi = 0.50$.

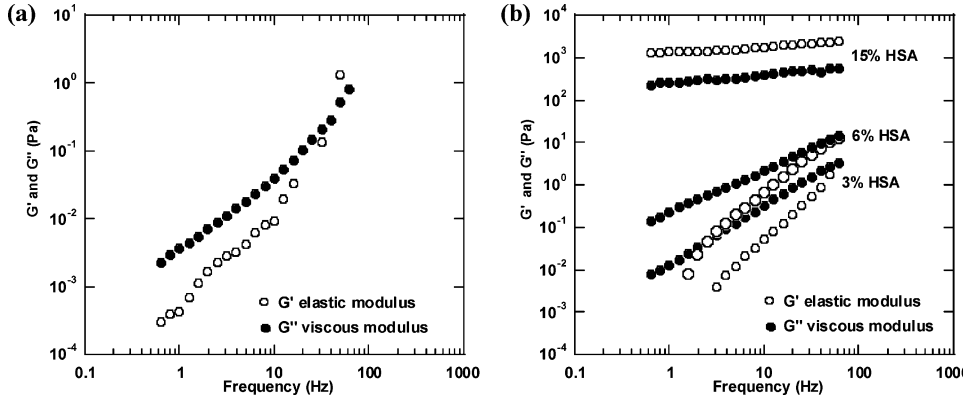

Figure 8. Elastic and viscous moduli for (a) the emulsion and (b) the dispersions of organogel particles with $\phi = 0.24$ at various organogelator contents in the oil phase: 3%, 6%, and 15% (25 °C).

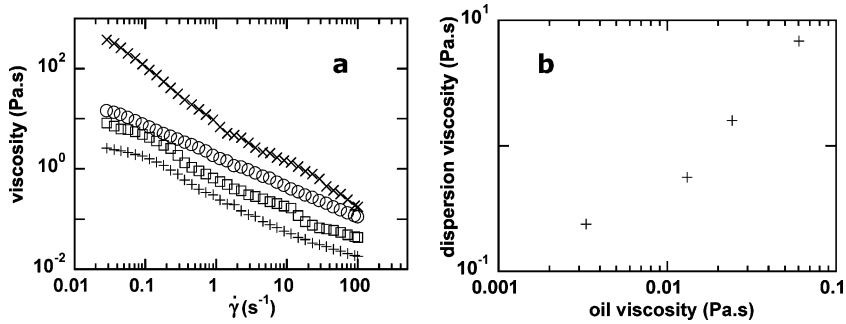

Figure 10. (a) Influence of the viscosity of the oil constituting the internal phase on the organogel dispersion flow viscosity: (+) dicaprylic ether; (□) dodecyl/pentadecyl benzoate; (○) caprylic/capric triglycerides; (×) soybean oil. (b) Flow viscosity curves of the organogel dispersions versus the viscosity of the oil at $\dot{\gamma} = 1$ s^{-1}. Conditions: $\phi = 0.24$; CTAB, 2%; HSA, 3%. All viscosity values are measured at 25 °C.

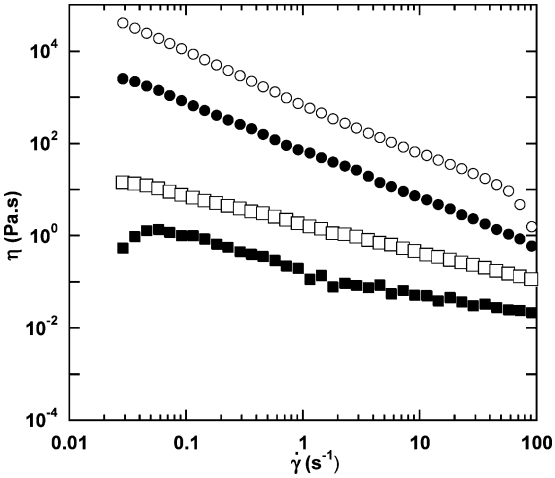

Figure 11. Influence of salt on the flow viscosity of the emulsion and the dispersion of organogel particles for $\phi = 0.50$ (25 °C). Emulsion (no HSA): (□) no salt and (■) [NaCl] = 0.15 mol·L^{-1}. Organogel particles (12% HSA): (○) no salt and (●) [NaCl] = 0.15 mol·L^{-1}.

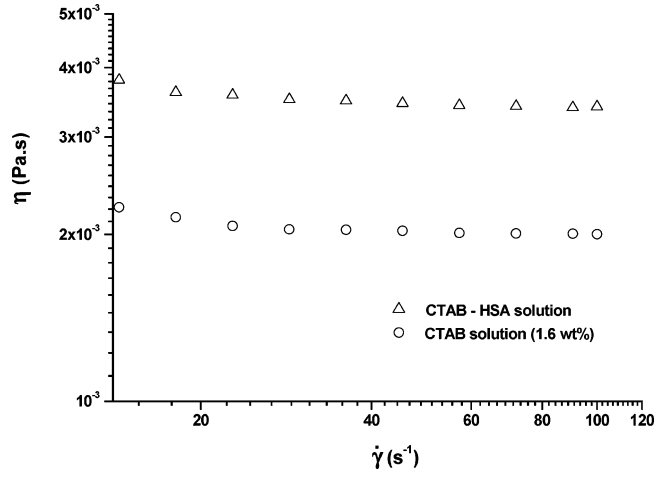

Figure 12. Influence of the CTAB and the CTAB/HSA mixture on flow curves (25 °C).

the effect of HSA on the rheology of the dispersions is not due only to the increase in the viscoelasticity of the droplets.

3.4. Influence of Other Parameters. ***3.4.1. Oil Viscosity.*** To investigate the influence of the viscosity of the dispersed phase, we used different oils: dicaprylic ether (3 10^{-3} Pa·s), alkyl benzoate (13 10^{-3} Pa·s), capric/caprylic triglycerides (24 10^{-3} Pa·s), and soybean oil (60 10^{-3} Pa·s). Figures 10a and 10b show the influence of the oil viscosity on the flow dispersion viscosity. The flow curves shown in Figure 10b were obtained for $\phi = 0.24$ and 3% HSA. Clearly, increase of the viscosity of the oil increased the overall viscosity of the suspensions. This indicates that, at this volume fraction, the viscoelastic properties of the droplets influenced the rheology of the dispersion.

3.4.2. Salt Effect. The influence of salt (NaCl 0.15 mol/L) on the dispersions of gelled droplets and on the emulsion was also investigated. Figure 11 gathers the results for the emulsion and the dispersion of gelled particles (12% HSA), both at $\phi = 0.50$. In both cases, the presence of salt significantly decreased the shear viscosity, most likely because the electrostatic repulsion between particles or droplets was screened by the ionic strength, reducing their effective volume. This confirms the role of electrostatic interactions proposed above to explain the relatively low maximum packing fraction (ϕ_m) determined for the emulsion.

3.5. Electron Microscopy and Result Interpretation. A first analysis of the rheological behavior of the dispersion of gelled particles could suggest that a fraction of HSA passes into the water phase, most likely within CTAB micelles, modifying the flow properties of the continuous phase. To test this hypothesis, we compared the viscosities between a solution of CTAB and the same solution saturated with HSA. The rheological behavior of solution containing 1.6 wt % of CTAB and of solution containing 1.6 wt % of CTAB and 15 wt % of HSA (see Figure 12) was studied in flow mode. Mixtures were heated at 75 °C (which is above the melting temperature of the HSA) in an oven for 20 min. Then, hot solutions (75 °C) were emulsified by sonication (20 kHz, 600 W) for 10 min and were cooled at room temperature after rheological measurements.The results indicate the same behavior, with a very small increase of viscosity in the case of HSA. Consequently, if the rheology of the continuous phase is not modified by HSA, interactions between gelled particles must be responsible for the increasing viscosity and the non-Newtonian behavior when the HSA content is increased.[49,50]

To understand and to confirm these possible interactions, we investigated the structure and the morphology of the gelled particles by different electron microscopy techniques. Freeze fracture electron microscopy (FF-TEM) confirmed the size and the morphology of these oily particles (see Figure 13a) but did not give any other information.[51−53] Transmission electron microscopy (TEM) in the presence of a staining agent (uranyl acetate) was more instructive (see Figure 13b−d).

The images clearly show contrast heterogeneities at the surface of the particles. Particulary large bright strips are observed (see Figure 13b). Interestingly, some images also show particles connected together by a kind of bright ribbon (see Figure 13c, d). These different observations could be helpful to explain the possible interactions between particles and their role on the rheological behavior of the dispersions.

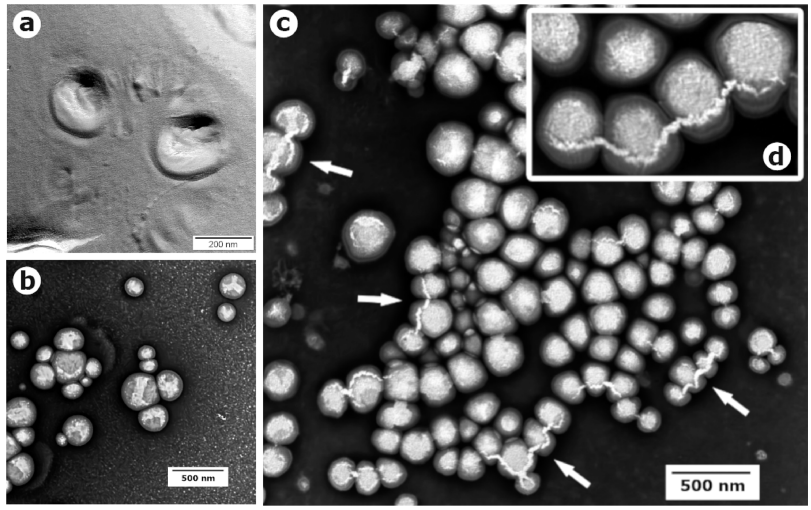

Figure 13. TEM micrographs of gelled nanoparticles: (a) FF-TEM; (b) TEM micrograph showing surface heterogeneities; (c) TEM micrograph with some bridged particles; (d) detail of bridged particles.

Before gelation, the system behaved like a classical emulsion composed of oil droplets stabilized by the surfactant molecules. When the temperature decreased below the T_{gel}, the gelation process took place with the formation of a 3D scaffold of fibrils inside the droplets. This phenomenon also had repercussions at the surface of the particle, with the formation of brighter areas corresponding perhaps to high-density zones of HSA fibrils. Moreover, this very high density of fibrils could desorb the surfactant molecules, leading to nonprotected areas favoring interactions between gelled particles. Some electron microscopy images show these kinds of interactions with several particles bridged on the surface by large ribbons of HSA fibrils (see Figure 13c, d). When two particles are sufficiently close, there is favorable surface self-assembling of the fibrils between each particle to link them by a ribbon of fibrils. Although these observations were made by TEM with a staining agent, and with strongly dehydrated samples, we think that it will be possible to extrapolate them to explain our rheological results in solution. We suggest that a proportion of bridged particles, even a very low one, could explain the rheological behavior of the dispersions and the influence of the amount of HSA on the viscosity.

4. Conclusion

We have conducted an unprecedented study of the rheological behavior of a new dispersed system consisting of organogel nanoparticles in water, stabilized by electrostatic repulsion. The rheology of these dispersions was compared with that of the equivalent emulsions, obtained either without gelling agent or at high temperature (above the T_{gel} of the organogel). The emulsion (without HSA) exhibited fairly standard behavior with a relatively high shear viscosity and low maximum packing fraction (ϕ_m) that was due to the small droplet size and the electrostatic stabilization. In comparison, the dispersions of organogel particles showed much higher values of the viscosity and of the elastic and viscous moduli, and a more pronounced shear-thinning behavior. Also, the evolution of the viscosity with the volume fraction did not fit into standard laws for dispersions of solid or liquid particles. There is also strong evidence that, at the higher volume fractions, the viscoelastic properties of the gelled particles influence the rheology of the dispersion. To explain these results, it is suggested that some bridged particles in solution could strongly affect the rheology of the dispersed phase. This hypothesis is based on TEM observations showing surface heterogeneities, possibly related to high and low density of HSA. High-density areas are not (or are only weakly) protected by the surfactant and could interact to connect some gelled particles by long ribbons of HSA fibers.

Acknowledgment. We gratefully thank Nacer Benmeradi (IBCG, UPS, Toulouse, France) for the TEM, Ghislaine Frébourg (SME, Pierre et Marie Curie University, Paris, France) for the FF-TEM images, and Pierre-Fabre Dermo-Cosmetic (Vigoulet Auzil, Toulouse, France) for financing the studies and providing the materials.

References and Notes

(1) Huang, X.; Weiss, R. *Tetrahedron* **2007**, *63*, 7375.
(2) Rogers, M. A.; Wright, A. J.; Marangoni, A. G. *Food Res. Int.* **2008**, *41*, 1026.
(3) van Bommel, K. J. C.; Shinkai, S. *Langmuir* **2002**, *18*, 4544.
(4) Sugiyasu, K.; Tamaru, S. I.; Takeuchi, M.; Berthier, D.; Huc, I.; Oda, R.; Shinkai, S. *Chem. Commun.* **2002**, *12*, 1212.
(5) Llusar, M.; Roux, C.; Pozzo, J. L.; Sanchez, C. *J. Mater. Chem.* **2003**, *13*, 2505.
(6) Dautel, O. J.; Lère-Porte, J. P.; Moreau, J. J. E.; Man, M. W. C. *Chem. Commun.* **2003**, *21*, 2662.
(7) George, M.; Weiss, R. G. *Acc. Chem. Res.* **2006**, *39*, 489.
(8) Abdallah, D. J.; Weiss, R. G. *Adv. Mater.* **2000**, *12*, 1237.
(9) Mercurio, D. J.; Spontak, R. J. *J. Phys. Chem. B.* **2001**, *105*, 2091.
(10) Terech, P.; Allegraud, J.; Garner, C. *Langmuir* **1994**, *10*, 3406.
(11) Yamasaki, S.; Tsutsumi, H. *Bull. Chem. Soc. Jpn.* **1995**, *68*, 123.
(12) Terech, P.; Pasquier, D.; Bordas, V.; Rossat, C. *Langmuir* **2000**, *16*, 4485.
(13) Moniruzzaman, M.; Sahin, A.; Winey, K. I. *Carbon* **2009**, *47*, 645.
(14) Lu, L.; Cocker, T. M.; Bachman, R. E.; Weiss, R. G. *Langmuir* **2000**, *16*, 20.
(15) Abdallah, D. J.; Weiss, R. G. *Langmuir* **2000**, *16*, 352.
(16) Lo Nostro, P.; Ramsch, R.; Fratini, E.; Lagi, M.; Ridi, F.; Carretti, E.; Ambrosi, M.; Ninham, B. W.; Baglioni, P. *J. Phys. Chem. B* **2007**, *111*, 11714.
(17) Stan, R.; Ciuculecu, D.; Franceschi-Messant, S.; Perez, E.; Rico-Lattes, I.; Lattes, A. *Rom. J. Chem.* **2005**, *50*, 695.
(18) Chen, W.; Yang, Y.; Lee, C. H.; Shen, A. Q. *Langmuir* **2008**, *24*, 10432.
(19) Lu, L.; Weiss, R. G. *Chem. Commun.* **1996**, *17*, 2029.
(20) Tamaru, S.; Nakamura, M.; Takeuchi, M.; Shinkai, S. *Org. Lett.* **2001**, *3*, 3631.
(21) Maitra, U.; Vijaykumar, P.; Chandra, N.; D'Souza, L. J.; Prasana, M. D.; Raju, A. R. *Chem. Commun.* **1999**, *7*, 595.
(22) Babu, P.; Sangeetha, N. M.; Vijaykumar, P.; Maitra, U.; Rissanen, K.; Raju, A. R. *Chem.—Eur. J.* **2003**, *9*, 1922–1932.
(23) Terech, P.; Gebel, G.; Ramasseul, R. *Langmuir* **1996**, *12*, 4321.

(24) Terech, P.; Scherer, C.; Demé, B.; Ramasseul, R. *Langmuir* **2003**, *19*, 10641.
(25) Xue, M.; Liu, H.; Peng, J.; Zhang, Q.; Fang, Y. *J. Colloid Interface Sci.* **2008**, *327*, 94.
(26) Weiss, R. G.; Terech, P. *Molecular Gels*; Springer: Dordrecht, The Netherlands, 2006.
(27) Terech, P.; Weiss, R. G. *Chem. Rev.* **1997**, *97*, 3133.
(28) Burkhardt, M.; Kinzel, S.; Gradzielski, M. *J. Colloid Interface Sci.* **2009**, *331*, 514.
(29) Lu, L.; Weiss, R. G. *Langmuir* **1995**, *11*, 3630.
(30) Mukkamala, R.; Weiss, R. G. *Langmuir* **1996**, *12*, 1474.
(31) Kirilov, P.; Lukyanova, L.; Franceschi,-Messant, S.; Perier, V.; Perez, E.; Rico-Lattes, I. *Colloids Surf., A* **2008**, *328*, 1.
(32) Kirilov, P; Franceschi-Messant, S.; Perez, E.; Rico-Lattes, I.; Bordat, P. WO Patent PCT/EP2007/060126, 2009.
(33) Mehnert, W.; Mäder, K. *Adv. Drug Delivery Rev.* **2001**, *47*, 165.
(34) Domb, A. J. *Int. J. Pharm.* **1995**, *124*, 271.
(35) Vintiloiu, A.; Leroux, J. C. *J. Controlled Release* **2008**, *125*, 179.
(36) Li, J. L.; Wang, R. Y.; Liu, X. Y.; Pan, H. H. *J. Phys. Chem. B* **2009**, *113*, 5011.
(37) Cappelaere, E.; Cressely, R.; Decruppe, J. P. *Colloids Surf., A* **1995**, *104*, 353.
(38) Larson, R. G. *The Structure and Rheology of Complex Fluids*; Oxford University Press: New York, 1999.
(39) Krieger, I. M. *Adv. Colloid Interface Sci.* **1972**, *3*, 111.
(40) Tadros, T. F. *Colloids Surf., A* **1994**, *91*, 39.
(41) Goller, M. I.; Obey, T. M.; Teare, D. O. H.; Vincent, B.; Wegener, M. R. *Colloids Surf., A* **1997**, *123−124*, 183.
(42) Gillies, G.; Prestidge, C. A.; Attard, P. *Langmuir* **2002**, *18*, 1674.
(43) Bhattacharya, S.; Pal, A. *J. Phys. Chem. B* **2008**, *112*, 4918.
(44) Matsumoto, Y.; Alam, M. M.; Aramaki, K. *Colloids Surf., A* **2009**, *341*, 27.
(45) Saiki, Y.; Prestidge, C. A. *KA Rheol. J.* **2005**, *17*, 191.
(46) Pal, R. *Chem. Eng. J.* **1997**, *67*, 37.
(47) Barnes, H. A. *Colloids Surf., A* **1994**, *91*, 89.
(48) Barnes, H. A.; Hutton, J. F.; Walters, K. *An Introduction to Rheology*; Elsevier Science Publishing Co., Copywrite; The Netherlands, 1989.
(49) Klinkesorn, U.; Sophanodora, P.; Chinachoti, P.; McClements, D. J. *J. Food Res. Int.* **2004**, *37*, 851.
(50) McClements, D. J. *Food Hydrocolloids* **2000**, *14*, 173.
(51) Liu, E. H.; Callaghan, P. T.; McGrath, K. M. *Langmuir* **2003**, *19*, 7249.
(52) Sakai, T.; Kamogawa, K.; Harusawa, F.; Momozawa, N.; Sakai, H.; Abe, M. *Langmuir* **2001**, *17*, 251.
(53) Disanayaka, B.; Zhaon, C. L.; Winnik, M. A. *Langmuir* **1990**, *6*, 163.

JP905260S